

# Thermally Stimulated Luminescence Properties of Dy-doped $\text{CaYAl}_3\text{O}_7$ Single Crystals

Akihiro Nishikawa,\* Kensei Ichiba, Takumi Kato,  
Daisuke Nakauchi, Noriaki Kawaguchi, and Takayuki Yanagida

Nara Institute of Science and Technology, 8916-5 Takayama, Ikoma, Nara 630-0192, Japan

(Received October 29, 2024; accepted December 17, 2024)

**Keywords:** single crystal, dosimeter, Dy

In this study, we prepared  $\text{CaYAl}_3\text{O}_7$  single crystals doped with 0.1, 0.5, and 1.0% Dy by the floating zone method, and investigated their photoluminescence (PL) and thermally stimulated luminescence (TSL) properties. All samples showed the luminescence of  $\text{Dy}^{3+}$  at approximately 480, 570, 660, 750, and 830 nm in PL, and PL quantum yields ( $QYs$ ) were 3.9–45%. TSL glow curve measurements showed peaks at about 70 and 250 °C for the 0.1 and 0.5% Dy-doped samples, while the 1.0% Dy-doped sample had a peak only at around 70 °C. The 0.5% Dy-doped sample indicated the highest TSL intensity among all samples and linearity in the 1–1000 mGy range. The lower detection limit of the 0.5% Dy-doped sample was 1 mGy.

## 1. Introduction

Some passive-type dosimeters are composed of phosphors that can store energy from ionizing radiation and release it when externally stimulated. The luminescence mechanism is described as follows. When the dosimetric material is exposed to ionizing radiation, electron and hole pairs are generated inside it. These carriers are trapped in trap centers after moving through the material. Upon the application of thermal or optical stimulation, the trapped carriers are re-excited to the conduction band and recombined at luminescence centers, releasing energy as light. The luminescence obtained by thermal stimulation is called thermally stimulated luminescence (TSL) while that obtained by optical stimulation is called optically stimulated luminescence (OSL). The intensities of TSL and OSL are proportional to dose irradiation. Hence, dosimetric materials with TSL and OSL can measure integrated doses. These dosimetric materials require a wide detectable dose range, low fading, and high chemical stability.<sup>(1)</sup> Fading refers to the phenomenon where trapped carriers are re-excited at room temperature, which reduces TSL or OSL intensity at the time of readout. Furthermore, human-body equivalency is specifically required for measuring personal dosage.<sup>(2)</sup> The TSL and OSL materials are mainly composed of inorganic materials. Various materials, including  $\text{CaF}_2:\text{Dy}$ ,  $\text{Al}_2\text{O}_3:\text{C}$ ,  $\text{NaMgF}_3:\text{Eu}$ , and  $\text{LiF}:\text{Mg}$ , Ti, have been reported as typical dosimeters.<sup>(1,3)</sup> These materials play an important

---

\*Corresponding author: e-mail: [nishikawa.akihiro.nc6@ms.naist.jp](mailto:nishikawa.akihiro.nc6@ms.naist.jp)  
<https://doi.org/10.18494/SAM5429>

role in medical fields and dating applications.<sup>(4–9)</sup> In addition, new TSL and OSL materials are still being developed and studied to clarify mechanisms of processes in more detail such as trapping or detrapping for charge carriers.<sup>(10–15)</sup>

Single crystals of the melilite structure doped with rare-earth elements have been studied and considered for phosphor, laser, and scintillator applications.<sup>(16–20)</sup> A previous study revealed that Dy-doped  $\text{CaYAl}_3\text{O}_7$  single crystals, because of their melilite structure, have the potential for use as yellow light-emitting devices.<sup>(21)</sup> The emission wavelength of  $\text{Dy}^{3+}$  is suitable for the wavelength sensitivity of common photodetectors such as photomultiplier tubes and photodiodes. In addition, TSL materials doped with Dy as the luminescence center have also been used in practice. Therefore, a Dy-doped  $\text{CaYAl}_3\text{O}_7$  single crystal can be expected as a dosimeter using TSL. However, there are no reports about the TSL properties of the Dy-doped  $\text{CaYAl}_3\text{O}_7$  single crystal. Against the above background, we synthesized  $\text{CaYAl}_3\text{O}_7$  single crystals doped with 0.1, 0.5, and 1.0% Dy, and investigated their TSL glow curves and dose-response function to evaluate dosimetric performance. Furthermore, we examined the effect of Dy concentration on the TSL properties.

## 2. Materials and Methods

### 2.1 Sample preparation

Dy-doped  $\text{CaYAl}_3\text{O}_7$  single crystals were made by the floating zone (FZ) method. The starting materials used were CaO (4N, Furuuchi Chemical Corporation),  $\text{Y}_2\text{O}_3$  (4N, Furuuchi Chemical Corporation),  $\text{Al}_2\text{O}_3$  (4N, Kojundo Chemical Laboratory Corporation), and  $\text{Dy}_2\text{O}_3$  (4N, Furuuchi Chemical) powders. The concentrations of Y as Dy ions were 0.1, 0.5, and 1.0%. The powders were mixed in an agate mortar. The mixed powders were formed into a rod by hydrostatic pressing, then sintered for 8 h in air at 1200 °C. An optical FZ furnace (Canon Machinery, FZD0192) with two halogen lamps was used to grow crystals. The obtained samples were mechanically polished.

### 2.2 Measurement method

To confirm the phase of the obtained samples, powder X-ray diffraction (XRD) patterns were measured using MiniFlex 600 (Rigaku). As for photoluminescence (PL) properties, Quantaaurus-QY (C11347, Hamamatsu Photonics) and Quantaaurus-Tau (C11367, Hamamatsu Photonics) were used to measure PL quantum yields ( $QYs$ ), a PL excitation/emission map, and PL lifetimes. TSL glow curves were obtained with our original setup consisting of an electric heater (SCR-SHQ-A, Sakaguchi E.H Voc) and a photomultiplier tube (H11890-01, Hamamatsu Photonics). The TSL glow curves were measured after all samples were irradiated with 1 Gy by an X-ray generator (XRB80N100/CB, Spellman), and the heating rate was 1 °C/s. The dose-response function was obtained using the same setup as that for the TSL glow curves.

### 3. Results and Discussion

Figure 1 shows the appearance and XRD patterns of all samples. All samples were colorless and transparent. The obtained XRD patterns were consistent with the  $\text{CaYAl}_3\text{O}_7$  melilite structure with the space group  $P\bar{4}2_1m$  according to reference data of ICSD: 039891. No clear peaks originating from impurity phases were observed in any of the samples. We concluded that all samples were  $\text{CaYAl}_3\text{O}_7$  single crystals successfully doped with Dy. However, peak intensity ratio showed some change with Dy concentration. This might be partly because the sample was not uniformly ground before the XRD measurement. The  $\text{CaYAl}_3\text{O}_7$  single crystal has a three-dimensional structure in which  $\text{Ca}^{2+}$  and  $\text{Y}^{3+}$  ions connect  $(\text{Al}_3\text{O}_7)^{5-}$  layers, and  $\text{Ca}^{2+}$  and  $\text{Y}^{3+}$  ions are located randomly in a 1:1 ratio.<sup>(18,21,22)</sup> It has been reported that when Dy is doped, the positions of  $\text{Ca}^{2+}$  and  $\text{Y}^{3+}$  ions would likely be replaced by  $\text{Dy}^{3+}$ .<sup>(17,21)</sup>

Figure 2(a) shows the PL emission/excitation map of the 0.5% Dy-doped sample. The results for only the 0.5% Dy-doped sample are presented in Fig. 2(a) because all samples exhibited similar behaviors. The luminescence was observed at around 480, 570, 660, 750, and 830 nm.

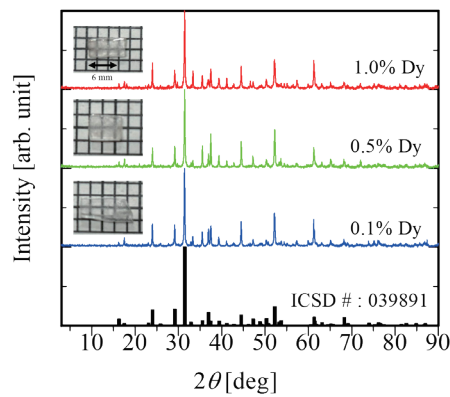


Fig. 1. (Color online) Appearance and XRD patterns of all samples.

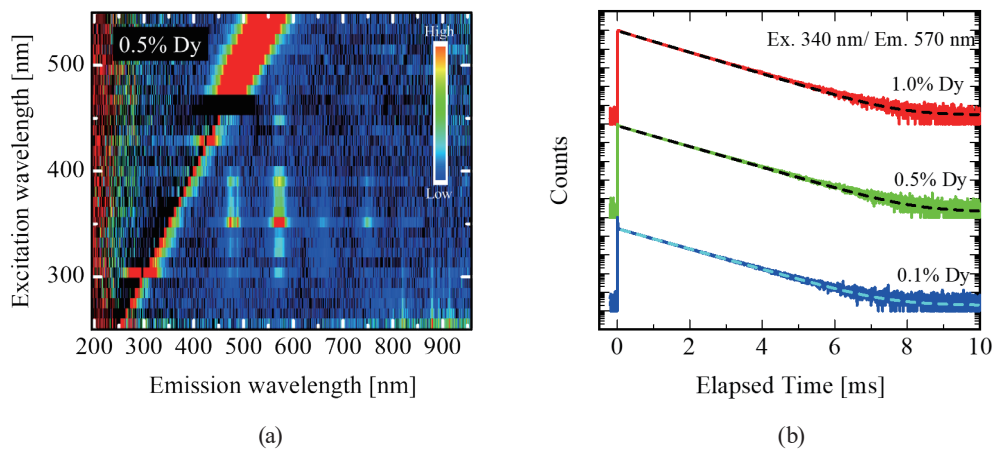


Fig. 2. (Color online) (a) PL emission/excitation map of the 0.5% Dy-doped sample. (b) PL decay curves of all samples.

The  $QY$ s monitored with an excitation wavelength of 350 nm are listed in Table 1. The  $QY$ s increased from 3.9 to 45% with Dy concentration. Figure 2(b) shows the PL decay curves of all samples. The decay curves were consistent with a single exponential component. The lifetimes calculated from the decay curves are also shown in Table 1, with values of around 800  $\mu$ s. The luminescences observed at approximately 480, 570, 660, 750, and 830 nm correspond to the transitions of  $Dy^{3+}$ , specifically,  ${}^4F_{9/2} \rightarrow {}^6H_{15/2}$ ,  ${}^6H_{13/2}$ ,  ${}^6H_{11/2}$ ,  ${}^6H_{9/2}$ , and  ${}^6H_{7/2}$ , respectively.<sup>(23–26)</sup> The measured lifetimes were consistent with those typically observed for  $Dy^{3+}$ .<sup>(27–30)</sup> Thus, we confirmed the presence of  $Dy^{3+}$  luminescence in the  $CaYAl_3O_7$  single crystals.

Figure 3(a) shows the TSL glow curves of all samples. All samples exhibited a peak at approximately 70  $^{\circ}C$ , while the 0.1 and 0.5% Dy-doped samples also displayed a broad peak at around 250  $^{\circ}C$ . The peak intensity at 250  $^{\circ}C$  increased with Dy concentration up to 0.5%, but the peak disappeared in the 1.0% Dy-doped sample. This suggested that adding up to 0.5% Dy might promote the formation of certain defects, whereas adding 1% Dy or more might work to compensate these defects. Among all the samples, the 0.5% Dy-doped sample showed the highest TSL intensity. The sharp increase in TSL intensity at around 350–400  $^{\circ}C$  was attributed to black-body radiation. We measured the dose-response function of the 0.5% Dy-doped sample, which had the highest TSL intensity. The integrated TSL intensity from 0 to 350  $^{\circ}C$  was used to determine the dose-response function. Additionally, the integrated TSL intensity from 150 to 350  $^{\circ}C$ , excluding the glow peak at around 0–150  $^{\circ}C$ , was also used for dose-response analysis. This exclusion is due to the possibility that the glow peak near 0–150  $^{\circ}C$  is strongly affected by fading. In both dose-response functions, the 0.5% Dy-doped sample demonstrated linearity in the 1–1000 mGy range, with a lower detection limit of 1 mGy.

Table 1  
 $QY$ s and lifetimes of all samples.

Dy concentration (%)	$QY$ (%)	Lifetime ( $\mu$ s)
0.1	3.9	800
0.5	16	783
1.0	45	753

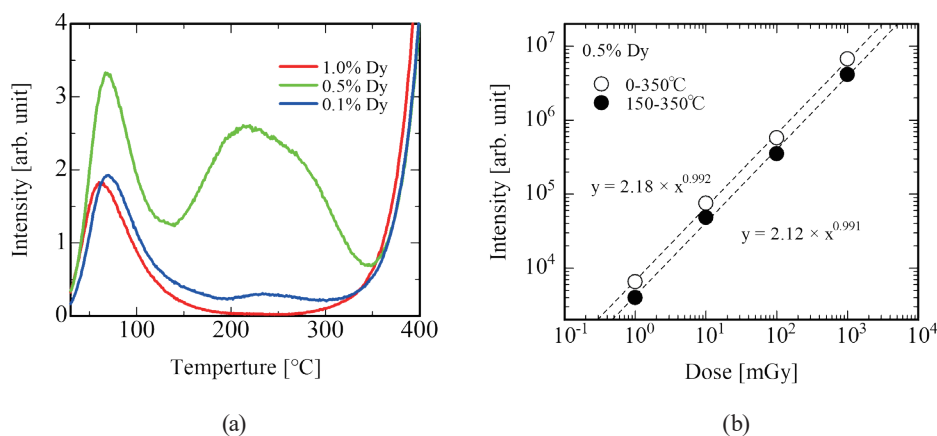


Fig. 3. (Color online) (a) TSL glow curves of all samples. (b) Dose-response function of the 0.5% Dy-doped sample.

## 4. Conclusions

We successfully synthesized CaYAl<sub>3</sub>O<sub>7</sub> single crystals doped with 0.1, 0.5, and 1.0% Dy. All samples exhibited luminescence derived from the 4f-4f transitions of Dy<sup>3+</sup> in PL. In the TSL glow curves, the 0.1 and 0.5% Dy-doped samples showed peaks at approximately 70 and 250 °C, while the 1.0% Dy-doped sample only exhibited a peak at around 70 °C. The 0.5% Dy-doped sample demonstrated the highest TSL intensity among all samples. To assess dosimetric performance, we measured the dose-response function. The 0.5% Dy-doped sample displayed good linearity in the 1–1000 mGy range, with a lower detection limit of 1 mGy. Therefore, the 0.5% Dy-doped CaYAl<sub>3</sub>O<sub>7</sub> single crystal showed potential for use as a TSL dosimeter.

## Acknowledgments

This work was supported by MEXT Grant-in-Aid for Scientific Research A (22H00309), Scientific Research B (23K21827, 23K25126 and 24K03197), Exploratory Research (22K18997), Early-Career Scientists (23K13689), JSPS Fellows (24KJ1699) from the Japan Society for the Promotion of Science, Nippon Sheet Glass Foundation, Terumo Life Science Foundation, KRF Foundation, Tokuyama Science Foundation, Iketani Science and Technology Foundation, Iwatani Naoji Foundation, and Foundation for Nara Institute of Science and Technology.

## References

- 1 H. Nanto and G. Okada: Jpn. J. Appl. Phys. **62** (2023) 010505. <https://doi.org/10.35848/1347-4065/ac9106>
- 2 T. Kato, D. Nakauchi, N. Kawaguchi, and T. Yanagida: Jpn. J. Appl. Phys. **62** (2023) 010604. <https://doi.org/10.35848/1347-4065/ac94ff>
- 3 Z. Yang, H. Vrielinck, L. G. Jacobsohn, P. F. Smet, and D. Poelman: Adv. Funct. Mater. **34** (2024) 1. <https://doi.org/10.1002/adfm.202406186>
- 4 G. W. Berger, A. S. Murray, K. J. Thomsen, and E. W. Domack: J. Geophys. Res. Earth Surf. **115** (2010) 1. <https://doi.org/10.1029/2009JF001415>
- 5 E. G. Yukihara, P. B. R. Gasparian, G. O. Sawakuchi, C. Ruan, S. Ahmad, C. Kalavagunta, W. J. Clouse, N. Sahoo, and U. Titt: Radiat. Meas. **45** (2010) 658. <https://doi.org/10.1016/j.radmeas.2009.12.034>
- 6 T. Rivera: Appl. Radiat. Isot. **71** (2012) 30. <https://doi.org/10.1016/j.apradiso.2012.04.018>
- 7 C. I. Burbidge, M. J. Trindade, M. I. Dias, L. Oosterbeek, C. Scarre, P. Rosina, A. Cruz, S. Cura, P. Cura, L. Caron, M. I. Prudêncio, G. J. O. Cardoso, D. Franco, R. Marques, and H. Gomes: Quat. Geochronol. **20** (2014) 65. <https://doi.org/10.1016/j.quageo.2013.11.002>
- 8 N. Zacharias, K. Beltsios, A. Oikonomou, A. G. Karydas, V. Aravantinos, and Y. Bassiakos: J. Non. Cryst. Solids **354** (2008) 761. <https://doi.org/10.1016/j.jnoncrysol.2007.07.082>
- 9 L. A. DeWerd: Application of Thermally Stimulated Luminescence, P. Bräunlich Eds. (Springer, Berlin, 1979) pp. 275–299.
- 10 T. Kato, H. Kimura, K. Okazaki, D. Nakauchi, N. Kawaguchi, and T. Yanagida: Sens. Mater. **35** (2023) 483. <https://doi.org/10.18494/SAM4137>
- 11 H. Ezawa, Y. Takebuchi, K. Okazaki, T. Kato, D. Nakauchi, N. Kawaguchi, and T. Yanagida: Sens. Mater. **36** (2024) 465. <https://doi.org/10.18494/SAM4757>
- 12 K. Ichiba, Y. Takebuchi, H. Kimura, T. Kato, D. Nakauchi, N. Kawaguchi, and T. Yanagida: Sens. Mater. **35** (2023) 475. <https://doi.org/10.18494/SAM4143>
- 13 S. Otake, H. Sakaguchi, Y. Yoshikawa, T. Kato, D. Nakauchi, N. Kawaguchi, and T. Yanagida: Sens. Mater. **36** (2024) 539. <https://doi.org/10.18494/SAM4759>
- 14 R. Tsubouchi, H. Fukushima, T. Kato, D. Nakauchi, S. Saijo, T. Matsuura, N. Kawaguchi, T. Yoneda, and T. Yanagida: Sens. Mater. **36** (2024) 481. <https://doi.org/10.18494/SAM4763>

- 15 M. Koshimizu, K. Oba, Y. Fujimoto, and K. Asai: *Sens. Mater.* **36** (2024) 565. <https://doi.org/10.18494/SAM4761>
- 16 C. J. Yim, S. Unithrattil, W. J. Chung, and W. Bin Im: *Mater. Charact.* **95** (2014) 27. <https://doi.org/10.1016/j.matchar.2014.06.002>
- 17 Y. Li, Z. Jia, H. Nie, Y. Yin, X. Fu, W. Mu, J. Zhang, B. Zhang, S. Li, and X. Tao: *CrystEngComm* **22** (2020) 4723. <https://doi.org/10.1039/D0CE00730G>
- 18 Y. Li, Z. Jia, Y. Yin, Q. Hu, W. Mu, J. Zhang, X. Yu, and X. Tao: *J. Alloys Compd.* **748** (2018) 57. <https://doi.org/10.1016/j.jallcom.2018.03.089>
- 19 K. Igashira, D. Nakauchi, Y. Fujimoto, T. Kato, N. Kawaguchi, and T. Yanagida: *Opt. Mater.* **102** (2020) 109810. <https://doi.org/10.1016/j.optmat.2020.109810>
- 20 S. Vandana and C. Joseph: *J. Phys. Conf. Ser.* **2070** (2021) 012097. <https://doi.org/10.1088/1742-6596/2070/1/012097>
- 21 W. Zhang, H. Shen, X. Hu, Y. Wang, J. Li, Z. Zhu, Z. You, and C. Tu: *J. Alloys Compd.* **781** (2019) 255. <https://doi.org/10.1016/j.jallcom.2018.12.113>
- 22 Y. Zhang, X. Yin, H. Yu, H. Cong, H. Zhang, J. Wang, and R. I. Boughton: *Cryst. Growth Des.* **12** (2012) 622. <https://doi.org/10.1021/cg2007205>
- 23 Z. Yang, C. Ji, G. Zhang, G. Han, H. Wang, H. Bu, D. Xu, and J. Sun: *J. Mater. Sci. Mater. Electron.* **29** (2018) 12632. <https://doi.org/10.1007/s10854-018-9380-x>
- 24 M. S. Rabasovic, D. Sevic, J. Krizan, M. D. Rabasovic, S. Savic-Sevic, M. Mitric, M. Petrovic, M. Gilic, and N. Romcevic: *Opt. Mater.* **50** (2015) 250. <https://doi.org/10.1016/j.optmat.2015.11.002>
- 25 M. Higuchi, R. Sasaki, and J. Takahashi: *J. Cryst. Growth* **311** (2009) 4549. <https://doi.org/10.1016/j.jcrysgro.2009.08.02>
- 26 A. Strzyp, I. R. Martin, M. Głowacki, W. Ryba-Romanowski, M. Berkowski, and C. Pérez-Rodríguez: *J. Lumin.* **166** (2015) 304. <https://doi.org/10.1016/j.jlumin.2015.05.013>
- 27 R. Zhu, J. Dong, Z. Lin, and Z. Lin: *J. Lumin.* **245** (2022) 118787. <https://doi.org/10.1016/j.jlumin.2022.118787>
- 28 Y. Zhang, J. Xu, and B. Lu: *J. Alloys Compd.* **582** (2014) 635. <https://doi.org/10.1016/j.jallcom.2013.08.090>
- 29 Y. Liu, F. Pan, C. Tu, and J. Gao: *J. Lumin.* **236** (2021) 118122. <https://doi.org/10.1016/j.jlumin.2021.118122>
- 30 E. Cavalli, E. Bovero, and A. Belletti: *J. Phys.: Condens. Matter* **14** (2002) 317. <https://doi.org/10.1088/0953-8984/14/20/317>